Inorganic Chemistry

ARTICLE

pubs.acs.org/IC

The Thermal Stabilities of Luminescence and Microstructures of Eu^{2+}-Doped $KBaPO_4$ and $NaSrPO_4$ with β-K_2SO_4 Type Structure

Suyin Zhang,[†] Yosuke Nakai,[‡] Taiju Tsuboi,[‡] Yanlin Huang,[†,*] and Hyo Jin Seo[§,*]

[†]College of Chemistry, Chemical Engineering and Materials Science, Soochow University, Suzhou 215123, China

[‡]Faculty of Engineering, Kyoto Sangyo University, Kamigamo, Kyoto 603-8555, Japan

[§]Department of Physics, Pukyong National University, Busan 608-737, Republic of Korea

Supporting Information

ABSTRACT:

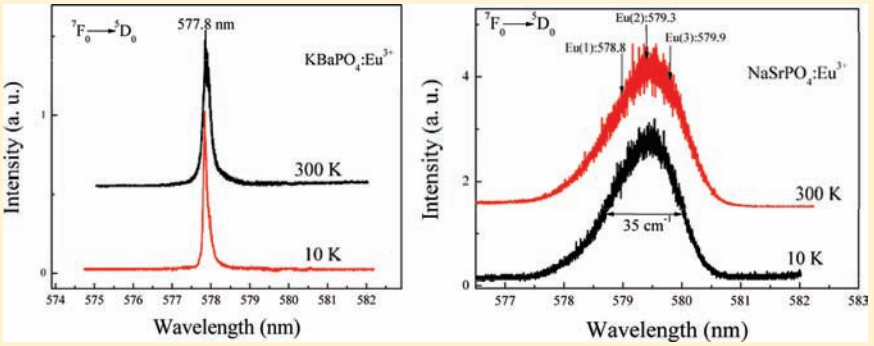

Eu^{2+}-doped monophosphates $NaSrPO_4$ and $KBaPO_4$ with the β-K_2SO_4 structure were synthesized using the conventional high temperature solid state reaction. The X-ray powder diffraction, photoluminescence excitation, and emission spectra and decay curves were measured. The phosphors can be efficiently excited by UV−visible light from 220 to 430 nm to realize emission in the visible range. The natures of the Eu^{2+} emission, e.g., the chromaticity coordinates, the Stokes shifts, and the luminescence absolute quantum efficiencies, were reported. The luminescence quenching temperatures and the thermal activation energies for $NaSrPO_4$:Eu^{2+} and $KBaPO_4$:Eu^{2+} were obtained from the temperature dependent (10−435 K) luminescence intensities and decay curves. $KBaPO_4$:Eu^{2+} presents only one emission center; however, Eu^{2+} ions have a "disordered environment" in $NaSrPO_4$ lattices. The relationship between the luminescence thermal stabilities and the crystal structures was discussed. The crystallographic occupations of rare earth ions doped in these hosts were analyzed by the site-selective emission spectra and the excitation spectra of Eu^{3+} ions in the $^7F_0 \rightarrow {}^5D_0$ transitions using a pulsed, tunable, and narrow-band dye laser. In $KBaPO_4$, the Eu^{3+} ions could be distributed in the host with a high "ordered state" in only one site in the lattices. However, the multiple site structure of Eu^{3+} ions with highly disordered distributions in $NaSrPO_4$ lattices was suggested.

1. INTRODUCTION

In recent years, rare earth (RE) activated inorganic compounds have been established as useful luminescent materials in fabricating optoelectronic devices. Nowadays, more and more interest has been focused on the synthesis and photoluminescence of the new RE doped compounds due to their potential applications.[1] Monophosphates with a tetrahedral rigid three-dimensional matrix have been given intense attention because of their excellent properties, e.g., the large band gap and the high absorption of PO_4^{3-} in the VUV region, moderate phonon energy, high chemical stability, and an exceptional optical damage threshold.[2]

The phosphates with the $ABPO_4$ formula (A and B are mono- and divalent cations, respectively) are in a large family of monophosphates with different structure types strictly depending on the relative size of the A and B ions.[3] The variety in these structures makes it possible to tailor the physical and chemical properties of the $ABPO_4$ materials.

Recently, Eu^{2+}-doped $ABPO_4$ with a β-K_2SO_4 structure has received much attention for potential applications as new white light emission diode (W-LED) phosphors.[4] Eu^{2+}-doped $KSrPO_4$ shows blue luminescence with better thermally stabilities than the commercial $Y_3Al_5O_{12}$:Ce^{3+} phosphor.[5] $KCaPO_4$:Eu^{2+}[6] and $NaCaPO_4$:Eu^{2+}[7] have been reported to be potential green-emitting W-LED phosphors. $KBaPO_4$:Eu^{2+} and $KSrPO_4$:Eu^{2+} show an emission band with a maximum at 420 and 430 nm, respectively.[8] Lin et al.[9] reported the full-color band phosphors, Eu^{2+}-, Tb^{3+}-, and Sm^{3+}-doped $KBaPO_4$, which could generate blue, green, and orange-red light, respectively.

Received: October 26, 2010
Published: February 28, 2011

The thermal stabilities of $KBaPO_4$:Ln (Ln = Eu^{2+}, Tb^{3+}, Sm^{3+}) are higher than those of the commercially available YAG:Ce^{3+}. $KBaPO_4$:Eu^{2+} coated by silica on the phosphor surface is very potent as a blue-emitting phosphor for PDPs (plasma display panels), CCFLs (cold cathode fluorescence lamps), and phosphor-converted (pc) W-LEDs based on near-ultraviolet LED.[10] Tung et al.[11] have reported that the blue-emitting $NaSr_{1-x}PO_4$:Eu_x exhibits a much higher emission intensity and better thermal stability under UV light excitation than the commercial ZnS:(Al, Ag) phosphors.

The wavelength positions of excitation and emission bands of Eu^{2+} ions strongly depend on the host crystal.[12] The luminescence thermal stabilities and efficiency of phosphors used in white W-LED are important. Dorenbos has proposed that the main mechanism responsible for the luminescence thermal quenching of Eu^{2+} in solids is the ionization of the electron from the lowest energy level of the relaxed Eu^{2+} $4f^65d^1$ electronic configuration to the host lattice conduction band level.[13] Lin et al.[4] recently suggested that the crystal structure and the coordination environment of activators at different temperatures could be responsible for the thermal stability.

The compounds $ABPO_4$ (A = Na^+, K^+ and B = Ca^{2+}, Sr^{2+}, Ba^{2+}; except for $NaBaPO_4$) have an isostructural type with β-K_2SO_4.[14] The important difference between these monophosphates and β-K_2SO_4 is that the latter has identical ions on the two different cation sites (K), whereas the monophosphates $ABPO_4$ have alkaline (A) and alkaline earth (B) ions on these sites.[15] The [PO_4] tetrahedra in $ABPO_4$ have to change their orientations so as to accommodate the coordination requirements of cations A and B.[16] This implies that the Eu^{2+}-doped $ABPO_4$ (A = Na^+, K^+ and B = Ca^{2+}, Sr^{2+}, Ba^{2+}) compounds have different microstructures, which can be ascribed to the orientation of [PO_4] in the lattices. This makes it useful to investigate the luminescence quenching effects on the different nonequivalent cation sites and distributions in $ABPO_4$ when A and B are changing in the lattices.

In this work, $Eu^{2+,3+}$-doped monophosphates $NaSrPO_4$ and $KBaPO_4$ with a β-K_2SO_4 structure have been selected to investigate the luminescence properties and thermal stabilities. X-ray powder diffraction (XRD), photoluminescence excitation and emission spectra, decay curves, and absolute luminescence quantum efficiency (QE) were measured. The activation energies for thermal quenching were obtained for $NaSrPO_4$:Eu^{2+} and $KBaPO_4$:Eu^{2+} from the temperature-dependent luminescence intensities and decay curves (10−435 K). The excitation spectra have been investigated in the $^7F_0 \rightarrow {}^5D_0$ region by using a pulsed, tunable, and narrow-band dye laser to detect Eu^{3+} ions sites in $NaSrPO_4$ and $KBaPO_4$. The occupation and the microstructure of Eu^{2+} and Eu^{3+} sites were discussed for $NaSrPO_4$ and $KBaPO_4$. This is helpful for further investigations about the luminescence of RE ions doped in phosphate hosts.

2. EXPERIMENTAL SECTION

Eu^{2+}-doped $NaSrPO_4$ and $KBaPO_4$ were synthesized using a conventional solid-state reaction. The starting material was a stoichiometric mixture of reagent grade $BaCO_3$, K_2CO_3, Na_2CO_3, $SrCO_3$, $(NH_4)_2HPO_4$ (A.R. grade), and Eu_2O_3 (99.99% purity). The doping level of Eu^{2+} is 3.0 mol %. First, the mixture was heated up to 350 °C over 10 h and kept at this temperature for 5 h. The obtained powder was mixed and then heated up to 750 °C for 5 h in the air. After that, the sample was thoroughly mixed and heated for 10 h in a reduction atmosphere (N_2/H_2 = 95:5) at 1050 °C. The samples of Eu^{3+}-doped $NaSrPO_4$ and $KBaPO_4$ were obtained by heating the as-prepared $NaSrPO_4$:Eu^{2+} and $KBaPO_4$:Eu^{2+} in an air atmosphere at 1000 °C for 5 h.

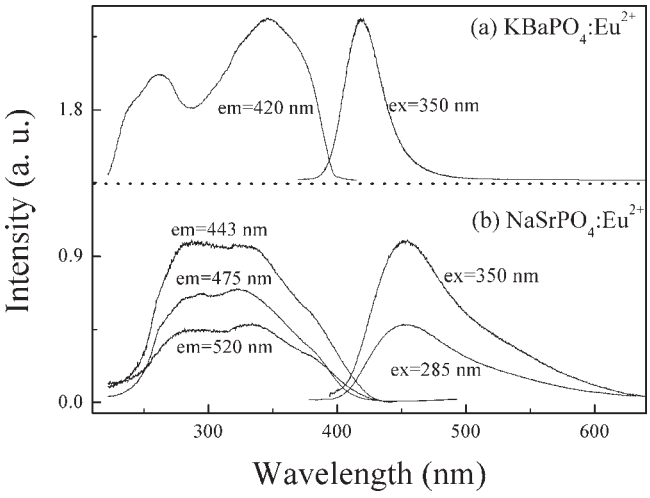

Figure 1. The photoluminescence spectra of $KBaPO_4$:Eu^{2+} (a) and $NaSrPO_4$:Eu^{2+} (b).

The XRD patterns were collected on a Rigaku D/Max diffractometer operating at 40 kV and 30 mA with Bragg−Brentano geometry using Cu Kα radiation (λ = 1.5405 Å). The photoluminescence excitation and emission spectra were recorded on a Perkin-Elmer LS-50B luminescence spectrometer with Monk−Gillieson type monochromators and a xenon discharge lamp used as an excitation source. Luminescence spectra were recorded between 10 and 300 K on a 75 cm monochromator (Acton Research Corp. Pro-750) equipped with a helium flow cryostat and observed with a photomultiplier tube (PMT; Hamamatsu R928). To study the thermal quenching from 20 to 500 °C, the same spectrofluorimeter was equipped with a home-made heating cell under the excitation of a 365 nm UV lamp. The luminescence decay was measured using the third harmonic (355 nm) of a pulsed Nd:YAG laser. The luminescence QEs was measured by an Absolute Photoluminescence Quantum Yield Measurement System (C9920-02, Hamamatsu) at room temperature. The excitation was performed by changing the excitation wavelength of light from 150 W Xe-lamp.

The excitation spectra of the $^7F_0 \rightarrow {}^5D_0$ transition of Eu^{3+} were obtained by monitoring the total luminescence by setting the monochromator in zero order of diffraction to pass all of the $^5D_0 \rightarrow {}^7F_J$ (J = 1, 2, 3 and 4) emission, in which a 580 nm cutoff filter was used. The excitation source was a dye laser (Spectron Laser Sys. SL4000) pumped by the second harmonic (532 nm) of a pulsed Nd:YAG laser (Spectron Laser Sys. SL802G). The pulse energy was about 5 mJ with a 10 Hz repetition rate and 5 ns duration. The luminescence was dispersed by a 75 cm monochromator (Acton Research Corp. Pro-750) and observed with a photomultiplier tube (Hamamatsu R928). Suitable filters were used to eliminate the intense laser scattering.

3. RESULTS AND DISCUSSIONS

3.1. The Photoluminescence Spectra. The photoluminescence excitation and emission spectra of $KBaPO_4$:Eu^{2+} and $NaSrPO_4$:Eu^{2+} are shown in Figure 1. The excitation spectra show broad absorption from 200 to 430 nm, which can be attributed to the 4f−5d transition of Eu^{2+} ions. This suggests that the phosphors can be effectively excited by UV LED chips (360−400 nm). This is necessary for potential applications in the

dx.doi.org/10.1021/ic102504x |Inorg. Chem. 2011, 50, 2897–2904

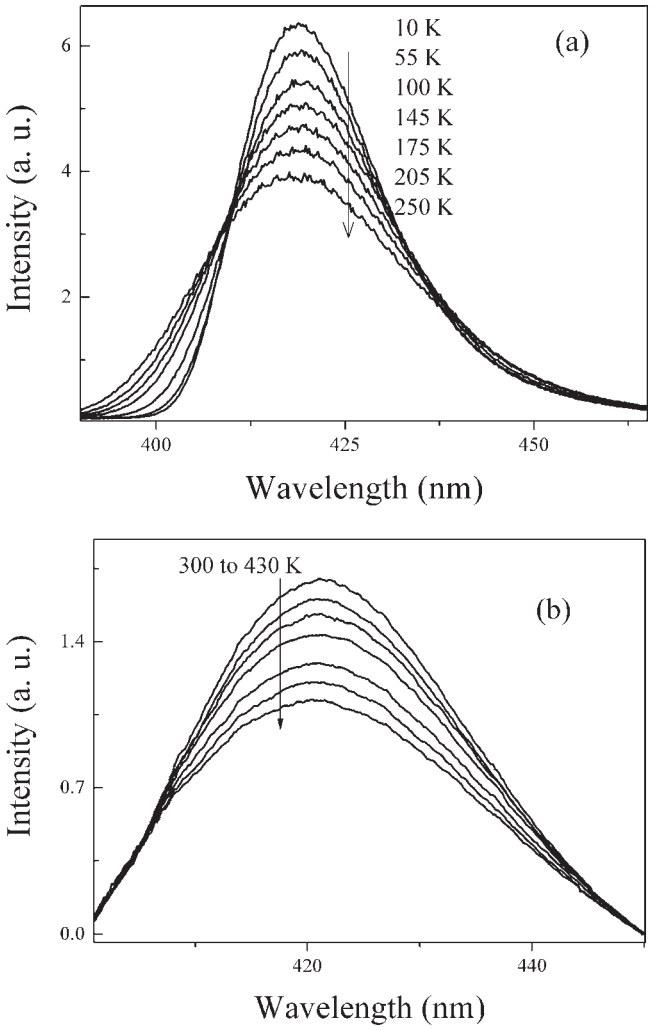

Figure 2. The emission spectra of $KBaPO_4:Eu^{2+}$ at different temperatures: (a) 10−250 K and (b) 300−430 K.

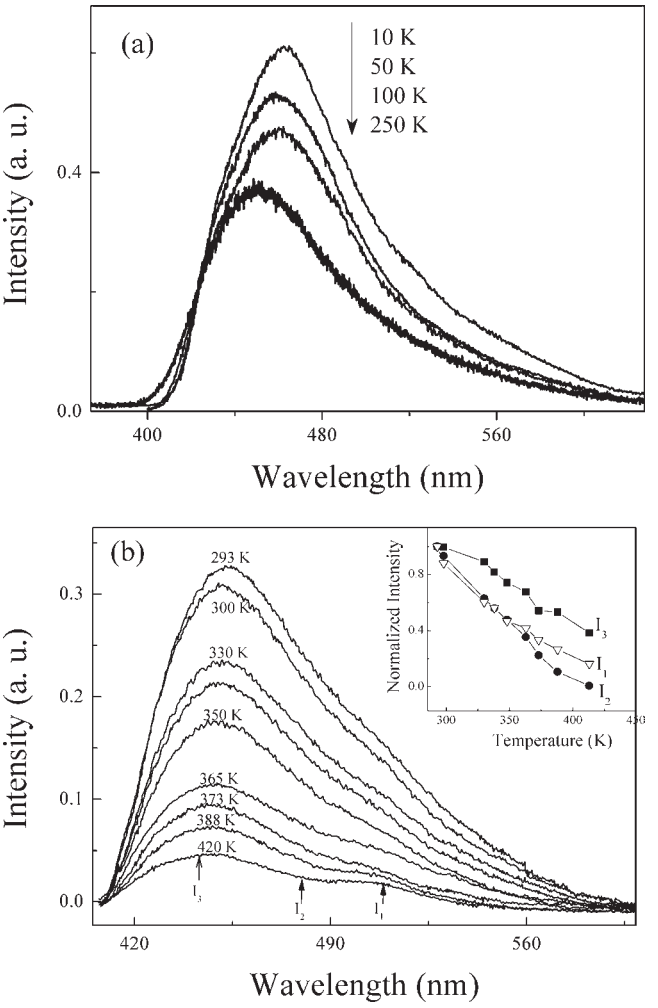

Figure 3. The emission spectra of $NaSrPO_4:Eu^{2+}$ at different temperatures: (a) 10−250 K and (b) 300−420 K. The inset in part b is the decreasing of normalized intensities for three luminescence bands.

W-LEDs fabricated with near-UV chips. This result agrees with what was reported for $KBaPO_4:Eu^{2+}$[8,9] and $NaSrPO_4:Eu^{2+}$.[11] On the emission spectrum of $KBaPO_4:Eu^{2+}$ (λ_{ex} = 350 nm), one emission band peaking at 420 nm is observed from the $4f^65d \rightarrow 4f^7$ ($^8S_{7/2}$) transitions in Eu^{2+} ions. The full width at half-maximum (fwhm) of the emission is 1900 cm^{-1}. The corresponding Stokes shift of $KBaPO_4:Eu^{2+}$ can be evaluated to be 3500 cm^{-1}. Under the excitation of 350 and 285 nm, the emission spectra of $NaSrPO_4:Eu^{2+}$ consist of broad bands from 410 to 650 nm with a maximum wavelength at about 480 nm, which can be ascribed to a $5d \rightarrow 4f$ allowed transition of Eu^{2+} ions.

Under the excitation of UV light, $KBaPO_4:Eu^{2+}$ presents a bright blue luminescence with CIE (Commission Internationale de l'Eclairage) color coordinates of $x = 0.18$, $y = 0.11$, and $NaSrPO_4:Eu^{2+}$ shows a white light having CIE color coordinates $x = 0.22$, $y = 0.23$. Under the same experimental conditions, the luminescence intensity of $KBaPO_4:Eu^{2+}$ is 1.4 times higher than that of $NaSrPO_4:Eu^{2+}$ phosphor (the emission spectra and CIE as shown in the Supporting Information S1). The absolute QE of a phosphor is important for its application. The luminescence QEs of $KBaPO_4:Eu^{2+}$ and $NaSrPO_4:Eu^{2+}$ were measured to be 47.9% and 34.2%, respectively, at the excitation of 330 nm light.

3.2. The Thermal Quenching of the Eu^{2+} Emission. In general, the temperature dependence of W-LED phosphors is important because it has great influence on the light output and color rendering index. Phosphors must sustain emission efficiency at temperatures of about 150 °C over a long term when they are used in W-LEDs. It is thus required that the thermal quenching of phosphors should be small, typically for high-power ones.

The luminescence thermal quenching effects of $KBaPO_4:Eu^{2+}$ and $NaSrPO_4:Eu^{2+}$ were evaluated by measuring the temperature-dependent emission intensities as shown in Figures 2 and 3, respectively. The emission intensities of Eu^{2+} decrease with an increase in temperature. The luminescence decays were measured as a function of the temperature for $KBaPO_4:Eu^{2+}$ and $NaSrPO_4:Eu^{2+}$, shown in Figure 4. The luminescence decay curves of $KBaPO_4:Eu^{2+}$ show exponential properties (Figure 4a), which can be fitted by a single-exponential function as

$$I = A \exp(-t/\tau) \quad (1)$$

where I is the phosphorescence intensity, A is a constant, t is the time, and τ is the decay time for the exponential component. Figure 4b shows the nonexponential curves of $NaSrPO_4:Eu^{2+}$ at

dx.doi.org/10.1021/ic102504x |Inorg. Chem. 2011, 50, 2897–2904

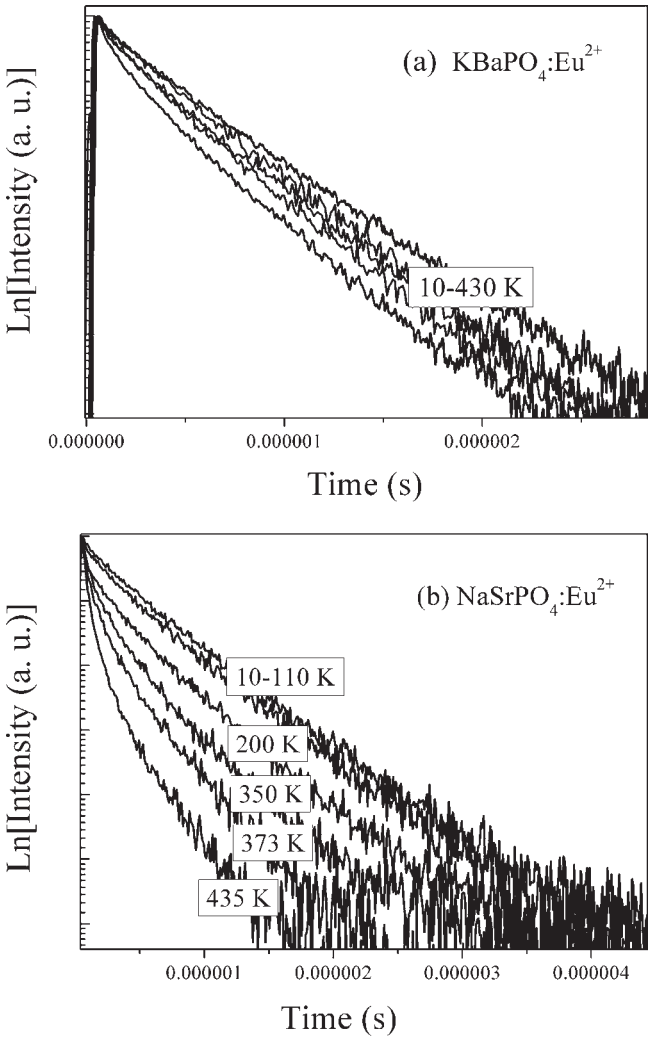

Figure 4. The luminescence decay curves of $KBaPO_4:Eu^{2+}$ (a) and $NaSrPO_4:Eu^{2+}$ (b) phosphors under an excitation of 355 nm of a pulsed Nd:YAG laser at different temperatures.

different temperatures, which can be fitted to the effective lifetime defined as follows:[17]

$$\tau_{\text{average}} = \frac{\int_0^\infty I(t)t\ \mathrm{d}t}{\int_0^\infty I(t)\ \mathrm{d}t} \qquad (2)$$

where $I(t)$ represents the luminescence intensity at a time t after the cutoff of the excitation light.

The luminescence decay lifetimes and the integrated emission intensities of $KBaPO_4:Eu^{2+}$ and $NaSrPO_4:Eu^{2+}$ as a function of the temperature are displayed in Figure 5. The thermal quenching of $KBaPO_4:Eu^{2+}$ begins during the heating at 140 K (Figure 5 a). The thermal quenching temperature, $T_{0.5}$, defined as the temperature at which the emission intensity is 50% of its original value, is about 500 K for $KBaPO_4:Eu^{2+}$ and 300 K for $NaSrPO_4:Eu^{2+}$. Compared with $KBaPO_4:Eu^{2+}$, $NaSrPO_4:Eu^{2+}$ has a relatively low quenching temperature. The temperature dependence of the intensity and the luminescence decay time remain nearly the same, both being affected in a similar manner by thermally induced nonradiative decay processes.

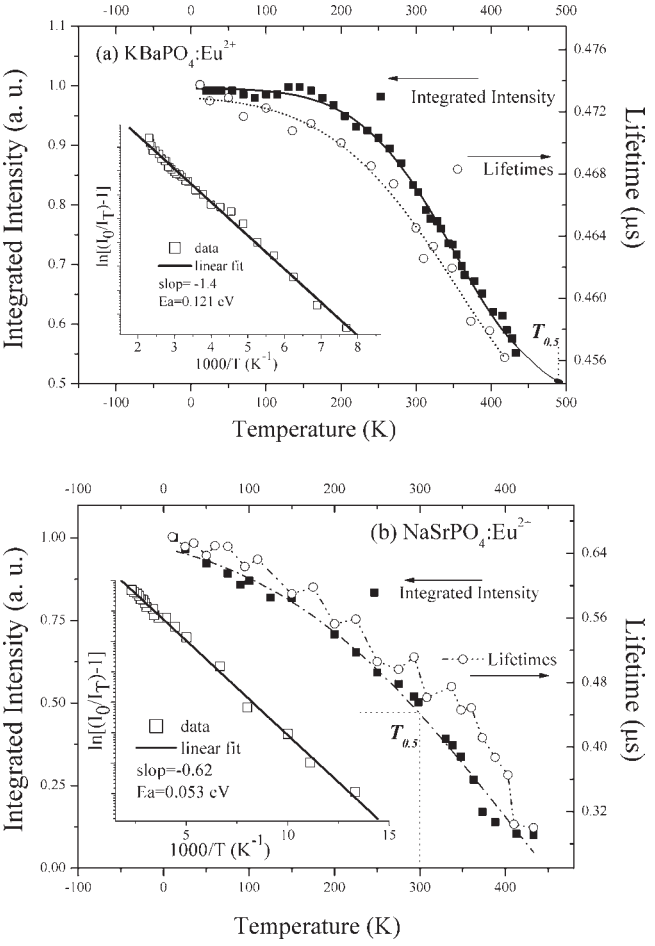

Figure 5. The temperature-dependent luminescence intensities and lifetimes of $KBaPO_4:Eu^{2+}$ (a) and $NaSrPO_4:Eu^{2+}$ (b) phosphors. The insets in the two parts show the activation energies of the thermal quenching fitted in eq 3.

The temperature dependence of the luminescence intensity of $KBaPO_4:Eu^{2+}$ and $NaSrPO_4:Eu^{2+}$ is described by a modified Arrhenius equation as follows:[18]

$$I_T = \frac{I_0}{1 + c\exp\left(-\frac{\Delta E}{kT}\right)} \qquad (3)$$

where I_0 is the initial emission intensity, I_T is the intensity at different temperatures, c is a rate constant for the thermally activated escape, E is the activation energy connected with this process (the energy gap between the lowest energy Eu^{2+} $4f^65d^1$-excited level and the bottom of the conduction band),[19] and k is the Boltzmann constant (8.629×10^{-5} eV). The inset in Figure 5 plots $\ln[(I_0/I_T) - 1]$ versus $1000/T$ for $KBaPO_4:Eu^{2+}$ and $NaSrPO_4:Eu^{2+}$. According to eq 3, the activation energies ΔE were calculated to be 0.121 eV for $KBaPO_4:Eu^{2+}$ and 0.053 eV for $NaSrPO_4:Eu^{2+}$.

It has been proposed that the main mechanism responsible for the thermal quenching of Eu^{2+} luminescence in solids is the ionization of the electron from the lowest energy level of the relaxed Eu^{2+} $4f^65d^1$ electronic configuration to the host lattice conduction band level.[20] This was confirmed by temperature-dependent photoconductivity experiments.[21] It was determined that thermal quenching due to level crossing in the single

dx.doi.org/10.1021/ic102504x |Inorg. Chem. 2011, 50, 2897–2904

configuration coordinate model cannot satisfactorily account for the variation in the thermal quenching temperature of the Eu^{2+} emission in solids.[13] Hence, the activation energy is the energy required to raise the electron from the relaxed excited level into the host lattice conduction band. The high $T_{0.5}$ and ΔE for the Eu^{2+} emission in $KBaPO_4$ imply that the lowest energy level of the Eu^{2+} $4f^6 5d^1$ electronic configuration is well isolated from the host lattice conduction band in comparison to that of $NaSrPO_4$:Eu^{2+}. Here, the low $T_{0.5}$ and ΔE for $NaSrPO_4$:Eu^{2+} do not indicate that the Eu^{2+} emission is from the impurity-trapped exciton level because the normal Eu^{2+} emission may quench at relatively low temperatures if the lowest energy level of $4f^6[^7F_0]5d^1$ electronic configuration is located close to conduction band.[13]

3.3. The Luminescence and Crystal Structures. As shown above, $KBaPO_4$:Eu^{2+} and $NaSrPO_4$:Eu^{2+} show different luminescence spectra and thermal quenching effects. Recently, Lin et al.[4] elucidated the luminescent intensity of activators of Eu^{2+}, Tb^{3+}, and Sm^{3+} doped in $ABPO_4$ phosphors at various temperatures and suggested that the crystal structure and the coordination environment of activators at different temperatures are responsible for the luminescence thermal stability of $ABPO_4$ phosphates. In this case, the microstructure and crystallographic surrounding of Eu^{2+} ions at Ba^{2+} and Sr^{2+} sites should be understood.

To investigate the structural changes, the XRD patterns of $KBaPO_4$:Eu^{2+} and $NaSrPO_4$:Eu^{2+} were compared with JCPD No. 33-1002 and No. 29-1193 (Supporting Information S2). In a comparison between the phosphors and the corresponding standard cards, the positions and intensities of the main peaks are the same. No impurity lines were observed, and all of the reflections could be well indexed to a $KBaPO_4$ and $NaSrPO_4$ single phase, respectively. The lattice parameters were calculated to be a = 7.711 Å, b = 5.669 Å, and c = 9.974 Å for $KBaPO_4$:Eu^{2+} and a = 20.425 Å, b = 5.431 Å, and c = 17.224 Å for $NaSrPO_4$:Eu^{2+}. The two phosphates have a structure related to the β-K_2SO_4 type, which is made up of two types of strings along the a axis. One string consists of alternating $[PO_4]$ tetrahedra and alkaline atoms (A). Another string is made up of only alkaline earth atoms (B) parallel to the a axis (the structure sketch maps shown in Supporting Information S3 and S4).[3,15]

In $KBaPO_4$, the unit cell consists of the following columns: A, $-K(1)O_9-P(1)O_4-K(1)O_9-P(1)O_4-$, and B, $-Ba(1)O_9-Ba(1)O_9-Ba(1)O_9-$.[14a] The framework is built with successive arrays of K atoms and $[PO_4]$ tetrahedra at the same height. The Ba and K atoms are surrounded by $[PO_4]$ tetrahedra in a very compact arrangement. The Ba^{2+} ions are located in a nine-coordinated cage with a symmetry mirror along the a direction (Supporting Information S3). When Eu^{2+} is incorporated into a $KBaPO_4$ host, it substitutes one of the Ba^{2+} sites. Consequentially, one Eu^{2+} emission band was observed in the emission spectra (Figure 1). The reduction of the distance between Eu^{2+} and the coordinating anions will be unfavorable since the site is already too large for Eu^{2+}. The small relaxation results in a small shift of the parabolas in the configurational coordinate diagram, which is reflected in the luminescence spectra by a small Stokes shift, narrow bands, and a high luminescence quenching temperature.

The structure of $NaSrPO_4$ is made up of strings A, $-Na(2)O_9-P(1)O_4-Na(1)O_9-P(2)O_4-Na(3)O_9-$, and B, $-Sr(3)O_8-Sr(2)O_8-Sr(1)O_8-Sr(3)O_8-$.[15] The Na^+ ions form zigzag edge-sharing chains with alternating $[PO_4]$ tetrahedra along the a axis, and the Sr^{2+} ions are located in chains with slight alternative displacements over the a axis (Supporting Information S4). There exist three different Na sites (Na1, Na2, and Na3) and three different Sr sites (Sr1, Sr2, and Sr3) in $NaSrPO_4$ lattices. It is possible for the Eu^{2+} ions to be statistically doped in the different sites in $NaSrPO_4$ lattices. This could be reflected in the emission spectrum of $NaSrPO_4$:Eu^{2+}, which shows an asymmetric spectrum shape (Figure 1), indicating more than one emission center in $NaSrPO_4$ lattices. However, the excitation spectra from monitoring the 443, 475, and 520 nm emissions in Figure 1 show no difference from each other; i.e., the emission spectra of $NaSrPO_4$:Eu^{2+} show no dependence on the excitation wavelengths. The reason may be that the Eu^{2+} ions in $NaSrPO_4$ have several excited states overlapped, and consequently they show the unresolved broad excitation spectra. However, this disordered multisite structure of Eu^{2+} ions doped in $NaSrPO_4$ can be explained by the temperature-dependent luminescence spectra.

First, with the increasing of temperature, the emission bands of $NaSrPO_4$:Eu^{2+} show an abnormal blue shift. In Figure 2, the wavelength of the maximum emission of $KBaPO_4$ has no obvious shifts with increasing temperatures. However, $NaSrPO_4$ shows obvious blue shifts (Figure 3). Generally, the photoluminescence spectrum shows characteristic temperature dependence: as the temperature increases, the emission peak shifts to lower energy (red shift).[22] This anomalous blue shift in Eu^{2+}-doped phosphors has been ascribed to thermally active phonon-assisted thermal back-energy transfer among multiple Eu^{2+} centers; for example, Kim et al.[22] reported similar blue shifts of the emission bands in Sr_2SiO_4:Eu^{2+} and Ca_2SiO_4:Eu^{2+}. In Ca_2SiO_4:Eu^{2+}, there are two centers for Eu^{2+}, the low-energy emission Eu(II) and high-energy Eu(I). At low temperatures, barrier $E1$ (EuI) can be overcome, and the low-energy emission (EuII) is dominant. At higher temperatures, thermal back-transfer over barrier $E2$ (EuII) is possible, and consequently the higher energy emission (EuI) is dominant. Thus, blue-shift behavior is observed with increasing temperature. It is reasonable that this mechanism is validated for $NaSrPO_4$:Eu^{2+} because of the possibility of more than one available Eu^{2+} site in the lattices.

Second, the intensities of the spectral compositions in $NaSrPO_4$:Eu^{2+} show different changes with increasing temperature. In Figure 3, the emission intensities of Eu^{2+} ions decrease with increasing temperatures; however, it is obvious that the emission intensities of three emission bands, as labeled in Figure 3b, have different changes. The emission band I_2 drops faster than I_1 and I_3. This indicates that there could be multiple sites of Eu^{2+} ions in the $NaSrPO_4$ lattices.

The influencing mechanism of temperature on emission in Eu^{2+}-doped phosphors is complicated. Im et al.[23] have suggested that in compounds with alkaline earth cations the Ba substitution on preferential Sr sites leads to the repulsion of Eu^{2+} ions on low-coordinated and smaller Sr sites and favors the thermal stability of the phosphor. Lin et al.[4] have reported that the microstructure and the coordination environment of activators can be responsible for the thermal stability of Eu^{2+} emission in $ABPO_4$ phosphates. Following this suggestion, it is reasonable that in $KBaPO_4$:Eu^{2+} and $NaSrPO_4$:Eu^{2+} the features for the different emission spectra and thermal stabilities could be due to a certain degree of microstructure disorder in the lattices. For example, in the disordered multisite structure of Eu^{2+} ions doped in $NaSrPO_4$, the excitation energy could distribute in a different way for the various sites; consequentially, the luminescence quenching could occur due to the "quenching centers" in the lattices.

In order to investigate the site occupation of a RE ion doped in $KBaPO_4$ and $NaSrPO_4$, the site-selective excitation and emission

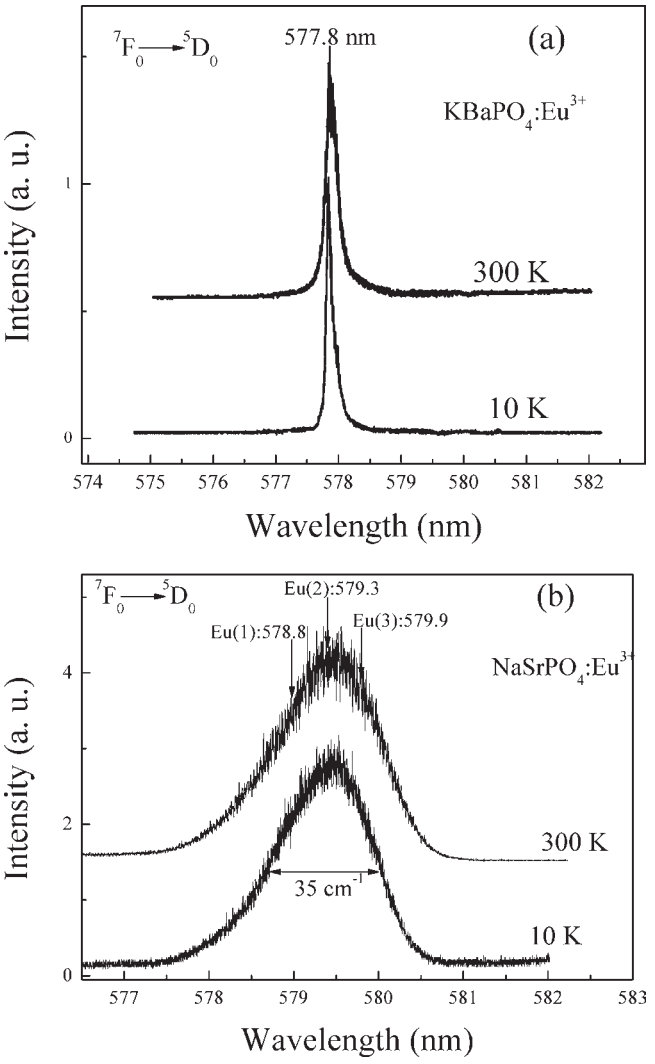

Figure 6. The excitation spectra for the $^7F_0 \rightarrow {}^5D_0$ transition of Eu^{3+} in $KBaPO_4:Eu^{3+}$ (a) and $NaSrPO_4:Eu^{3+}$ (b) at 10 and 300 K. The luminescences were monitored at the luminescence corresponding to $^5D_0 \rightarrow {}^7F_J$ (J = 1, 2, 3 and 4) by setting the monochromator at the zero wavelength position, and a 580 nm filter was used.

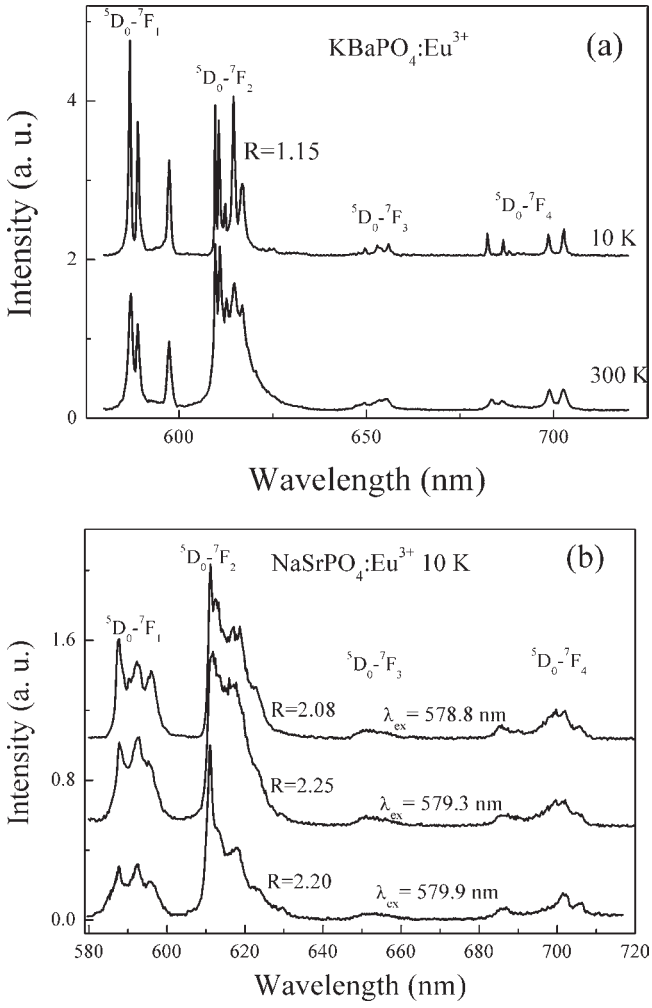

Figure 7. The site-selective emission spectra of $^5D_0 \rightarrow {}^7F_J$ (J =1, 2, 3, 4) transitions in $KBaPO_4:Eu^{3+}$ (a, exciting into 577.8 nm) and $NaSrPO_4:Eu^{3+}$ (b, exciting into 578.8 nm, 579.3 nm, and 579.9 nm).

spectra of Eu^{3+} ions were investigated. Usually, the presence of crystallographic nonequivalent sites in a host can be revealed by the structure probe Eu^{3+} ($4f^6$ configuration) because the emission and excitation lines between $^5D_0$ and $^7F_0$ levels are nondegenerate.[24]

3.4. The Site-Selective Excitation Spectra of Eu^{3+}. Figure 6a shows the excitation spectra for the $^7F_0 \rightarrow {}^5D_0$ transition, which is acquired by monitoring the total luminescence from Eu^{3+} in $KBaPO_4$ at 10 and 300 K, and shows only one narrow excitation peaking at 577.8 nm. This confirms that there is one crystallographic site for the Eu^{3+} ion in $KBaPO_4$. Figure 6b shows the excitation spectra for the $^7F_0 \rightarrow {}^5D_0$ transition from Eu^{3+} in $NaSrPO_4$ at 10 and 300 K, which are broad with large inhomogeneities.

Usually, the typical widths of the $^7F_0 \rightarrow {}^5D_0$ excitation transition are quite narrow, with a fwhm of less than 10 cm^{-1}.[25] In Figure 6b, the lines for the $^7F_0 \rightarrow {}^5D_0$ transition are much broader with a fwhm of 35 cm^{-1}. This could indicate that the Eu^{3+} ions occupy several disordered crystallographic sites, which could overlap with each other on the total excitation spectra. Suppose there are three Eu^{3+} sites on the base of the $NaSrPO_4$ structure (Figure 6), for example, $Eu^{3+}(1)$ at 578.8 nm, $Eu^{3+}(2)$ at 579.3 nm, and $Eu^{3+}(3)$ at 579.9 nm.

Figure 7 shows the site-selective emission spectra of $^5D_0 \rightarrow {}^7F_J$ (J = 1, 2, 3, 4) transitions of $KBaPO_4:Eu^{3+}$ and $NaSrPO_4:Eu^{3+}$ by tuning the laser to a resonance with each excitation peaks labeled in Figure 6a and b, respectively. The results clearly show one and three distinct europium spectra. This confirms there being one and three Eu^{3+} sites in $KBaPO_4:Eu^{3+}$ and $NaSrPO_4:Eu^{3+}$, respectively. It is well-known that site symmetry influences the $R = I(^5D_0 \rightarrow {}^7F_2)/I(^5D_0 \rightarrow {}^7F_1)$ intensity ratio, which corresponds to an "asymmetry" parameter. A lower symmetry of the crystal field around Eu^{3+} will result in a higher value of R.[26] The intensity ratio R of $KBaPO_4:Eu^{3+}$ is 1.15 (Figure 7a), which is quite smaller in comparison with those of the $NaSrPO_4:Eu^{3+}$ (2.08, 2.20, 2.25; Figure 7 b). This implies that the $Eu^{3+}(Ba)O_9$ in $KBaPO_4$ is not distorted. This result is consistent with the crystallographic results which show that the BaO_9 octahedron is quite regular with Eu−O bond lengths between 2.696 and 3.409 Å and O−Eu−O bond angles between 50.82° and 114.553° (Supporting Information S3). This also suggests that the Eu^{3+} ions in $NaSrPO_4$ are located in a heavily distorted cation environment relative to Eu^{3+} in $KBaPO_4$ lattices.

dx.doi.org/10.1021/ic102504x |*Inorg. Chem.* 2011, 50, 2897–2904

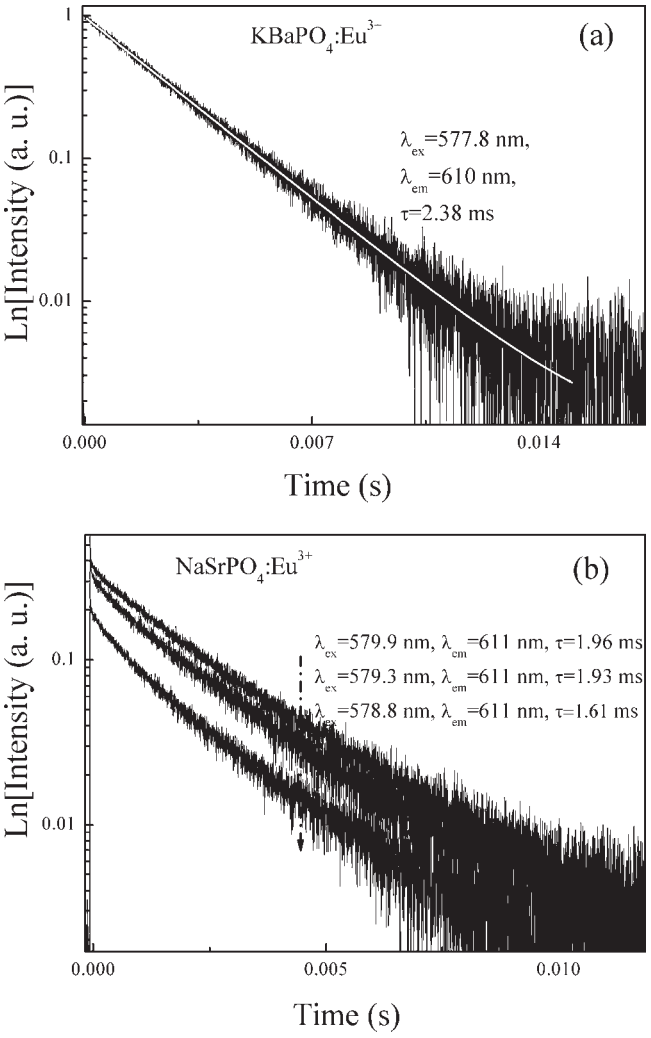

Figure 8. The $^5D_0 \rightarrow {}^7F_2$ luminescence decay curve of $KBaPO_4:Eu^{3+}$ (a) and $NaSrPO_4:Eu^{3+}$ (b) at 300 K.

Actually, this characteristic can be supported by the fluorescence decay curves for each site. For a given emitting ion, a long decay time is characteristic of the most symmetrical surrounding, while a short decay value can be observed when site distortion occurs.[27] Figure 8a shows decay curves of the $^5D_0 \rightarrow {}^7F_2$ emission under excitation in the Eu^{3+} site (577.8 nm) in $KBaPO_4$, which has a good exponential decay with a longer lifetime of 2.38 ms, fitted to eq 1. The luminescence decay curves of $^5D_0 \rightarrow {}^7F_2$ emission in $NaSrPO_4:Eu^{3+}$ under excitation in Eu(1) at 578.8 nm, Eu(2) at 579.3 nm, and Eu(3) sites at 579.9 nm (Figure 8b) display nonexponential curves, which can be fitted to eq 2. The luminescence lifetimes of the Eu^{3+} ions are calculated to be smaller (1.61−1.96 ms).

Similar to the excitation spectra in Figure 6b, the emission spectra of Eu^{3+} doped in $NaSrPO_4$ are broad with large inhomogeneities. Any broadening observed in the optical transition between the $^7F_0$ and $^5D_0$ levels reflects the bonding environments. The inhomogeneous broadening of the $^7F_0 \rightarrow {}^5D_0$ transition has a similar structure to that in glass matrices. This shows that the distributions of Eu(3), Eu(2), and Eu(1) in $NaSrPO_4$ are random and disordered. However, the excitation (Figure 6a) and emission spectra (Figure 7a) of Eu^{3+} ions doped in $KBaPO_4$ have very narrow shapes. This should be related to the more regular surroundings of Eu^{3+} ions, which correspond to its luminescence characteristics, for example, the long decay time and the smallest R value.

Certainly, the microstructure around Eu^{2+} and Eu^{3+} ions doped in $KBaPO_4$ and $NaSrPO_4$ could have some differences because of the different sizes and charge compensations even in the same host. However, from the luminescence characteristics of Eu^{2+} and the site-selective spectra of Eu^{3+} in the two hosts, it could be suggested that RE ions could be distributed in $KBaPO_4$ lattices at a high "ordered state" in only one site, and this was arranged in the "disordered multisite environment" over the whole structure in $NaSrPO_4$.

4. CONCLUSION

$KBaPO_4:Eu^{2+}$ and $NaSrPO_4:Eu^{2+}$ show a broad excitation band from 200 to 430 nm, which can be effectively excited by UV chips (360−400 nm) for potential applications in W-LEDs. $KBaPO_4:Eu^{2+}$ shows one emission band peaking at 420 nm. The emission spectra of $NaSrPO_4:Eu^{2+}$ have an asymmetric spectrum. The luminescence absolute QE of $KBaPO_4:Eu^{2+}$ (47.9%) is higher than that of $NaSrPO_4:Eu^{2+}$ phosphor (34.2%). The thermal quenching effects of $KBaPO_4:Eu^{2+}$ and $NaSrPO_4:Eu^{2+}$ were evaluated by measuring the temperature-dependent emission intensities and lifetimes. The thermal quenching temperatures $T_{0.5}$ for $KBaPO_4:Eu^{2+}$ and $NaSrPO_4:Eu^{2+}$ are 500 and 300 K, respectively. The activation energy ΔE is 0.121 eV for $KBaPO_4:Eu^{2+}$ and 0.053 eV for $NaSrPO_4:Eu^{2+}$. In $KBaPO_4$, Eu^{2+} ions have only one site distribution with a high "ordered state" in the lattices; however, in $NaSrPO_4$, Eu^{2+} sites were arranged in the "highly disordered environment" over the whole lattice. It is suggested that the microstructures of the Eu^{2+} distributions in a host have an obvious influence on the thermal quenching of the luminescence. In order to determine structure occupations for the RE doping in $KBaPO_4$ and $NaSrPO_4$, site-selective excitation and emission spectra of the $^7F_0 \rightarrow {}^5D_0$ transitions of Eu^{3+} ions were investigated. It could be suggested that RE ions could be doped in a high "ordered state" with only one site in $KBaPO_4$ lattices, and RE ions were arranged in the "disordered environment" over the whole structure in $NaSrPO_4$.

■ ASSOCIATED CONTENT

Supporting Information. The emission spectra of $KBaPO_4:Eu^{2+}$ and $NaSrPO_4:Eu^{2+}$ (b) under 365 nm excitation (Figure S1). XRD patterns of $KBaPO_4:Eu^{2+}$ and $NaSrPO_4:Eu^{2+}$ (Figure S2). Schematic structure of $KBaPO_4$ (Figure S3). Schematic structure of $NaSrPO_4$ (Figure S4). This material is available free of charge via the Internet at http://pubs.acs.org.

■ AUTHOR INFORMATION

Corresponding Author

*E-mail: hjseo@pknu.ac.kr (H.J.S.), huang@suda.edu.cn (Y.H.).

■ ACKNOWLEDGMENT

This work was supported by the Program for Postgraduates Research Innovation in University of Jiangsu Province (2010) in China and by the Midcareer Researcher Program through a National Research Foundation (NRF) grant funded by the

Ministry of Education, Science and Technology (MEST; Project No. 2009-0078682).

REFERENCES

(1) (a) Tanner, P. A.; Pan, Z. *Inorg. Chem.* **2009**, *48*, 11142–11146. (b) Logvinovich, D.; Arakcheeva, A.; Pattison, P.; Eliseeva, S.; Tomeš, P.; Marozau, I.; Chapuis, G. *Inorg. Chem.* **2010**, *49*, 1587–1594. (c) Cavalli, E.; Boutinaud, P.; Mahiou, R.; Bettinelli, M.; Dorenbos, P. *Inorg. Chem.* **2010**, *49*, 4916–4921. (d) Li, G.; Peng, C.; Li, C.; Yang, P.; Hou, Z.; Fan, Y.; Cheng, Z.; Lin, J. *Inorg. Chem.* **2010**, *49*, 1449–1457. (e) Zhang, L.; Jia, G.; You, H.; Liu, K.; Yang, M.; Song, Y.; Zheng, Y.; Huang, Y.; Guo, N.; Zhang, H. *Inorg. Chem.* **2010**, *49*, 3305–3309. (f) Li, W.; Tanner, P. A. *Inorg. Chem.* **2010**, *49*, 6384–6386. (g) Ana de Bettencourt-Dias, P. S.; Barber, S.; Viswanathan, D. T.; de Lill, A.; Rollett, G.; Ling, S. A. *Inorg. Chem.* **2010**, *49*, 8848–8861.

(2) (a) Kwon, K. H.; Im, W. B.; Jang, H. S.; Yoo, H. S.; Jeon, D. Y. *Inorg. Chem.* **2009**, *48*, 11525–11532. (b) Song, Y.; You, H.; Yang, M.; Zheng, Y.; Liu, K.; Jia, G.; Huang, Y.; Zhang, L.; Zhang, H. *Inorg. Chem.* **2010**, *49*, 1674–1678. (c) Yang, M.; You, H.; Liu, K.; Zheng, Y.; Guo, N.; Zhang, H. *Inorg. Chem.* **2010**, *49*, 4996–5002.

(3) Elammari, L.; Koumiri, M. El; Zschokke-Gränacher, I.; Elouadi, B. *Ferroelectrics* **1994**, *158*, 19–24.

(4) Lin, C. C.; Xiao, Z. R.; Guo, G. Y.; Chan, T. S.; Liu, R. S. *J. Am. Chem. Soc.* **2010**, *132*, 3020–3028.

(5) Tang, Y. S.; Hu, S. F.; Lin, C. C.; Nitin, C.; Liu, R. S. *Appl. Phys. Lett.* **2007**, *90*, 151108–151110.

(6) Zhang, S.; Huang, Y.; Seo, H. J. *J. Electrochem. Soc.* **2010**, *157* J261–J266.

(7) Qin, C.; Huang, Y.; Shi, L.; Chen, G.; Qiao, X.; Seo, H. J. *J. Phys. D: Appl. Phys.* **2009**, *42*, 185105–185109.

(8) Poort, S. H. M.; Janssen, W.; Blasse, G. *J. Alloys Compd.* **1997**, *260*, 93–97.

(9) Lin, C. C.; Tang, Y. S.; Hu, S. F.; Liu, R. S. *J. Lumin.* **2009**, *129* 1682–1684.

(10) Im, W. B.; Yoo, H. S.; Vaidyanathan, S.; Kwon, K. H.; Park, H. J.; Kim, Y. I.; Jeon, D. Y. *Mater. Chem. Phys.* **2009**, *115*, 161–164.

(11) Tung, Y. L.; Jean, J. H. *J. Am. Ceram. Soc.* **2009**, *92*, 1860–1862.

(12) (a) Dorenbos, P. *J. Lumin.* **2003**, *104*, 239–260. (b) Poort, S. H. M.; Blokpoel, W. P.; Blasse, G. *Chem. Mater.* **1995**, *7*, 1547–1551. (c) Bachmann, V.; Ronda, C.; Oeckler, O.; Schnick, W.; Meijerink, A. *Chem. Mater.* **2009**, *21*, 316–325.

(13) Dorenbos, P. *J. Phys.: Condens. Matter* **2005**, *17*, 8103–8111.

(14) (a) Masse, R.; Dufif, A. *J. Solid State Chem.* **1987**, *71*, 574–576. (b) Wyckoff, R. W. G. *Crystal Structures*, 2nd ed.; John Wiley and Sons: New York, 1965; Vol 3, p 95.

(15) Ben Amara, M.; Vlasse, M.; Le Flem, G.; Hagenmuller, P. *Acta Crystallogr., Sect. C* **1983**, *39*, 1483–1485.

(16) (a) Ben Amara, M. M.; Parent, C.; Vlasse, M.; Le Flem, G. *J. Solid State Chem.* **1983**, *46*, 321–327. (b) Ben Amara, M.; Parent, C.; Vlasse, M.; Le Flem, G.; Antic-Fidancev, E.; Piriou, B.; Caro, P. *J. Less Common Metals* **1983**, *93*, 425–429.

(17) Daldosso, M.; Falcomer, D.; Speghini, A.; Ghigna, P.; Bettinelli, M. *Opt. Mater.* **2008**, *30*, 1162–1167.

(18) Baginskiy, I.; Liu, R. S. *J. Electrochem. Soc.* **2009**, *156*, G29–G32.

(19) Bachmann, V.; Jüstel, T.; Meijerink, A.; Ronda, C.; Schmidt, P. J. *J. Lumin.* **2006**, *121*, 441–449.

(20) Kolk, E. v. d.; Dorenbos, P.; van Eijk, C. W. E.; Basun, S. A.; Imbusch, G. F.; Yen, W. M. *Phys. Rev. B* **2005**, *71*, 165120–165127.

(21) Happek, U.; Basun, S. A.; Choi, J.; Krebs, J. K.; Raukas, M. *J. Alloys Compd.* **2000**, *303−304*, 198–206.

(22) Kim, J. S.; Park, Y. H.; Kim, S. M.; Choi, J. C.; Park, H. L. *Solid State Commun.* **2005**, *133*, 445–448.

(23) Im, W. B.; Kim, Y. I.; Yoo, H. S.; Jeon, D. Y. *Inorg. Chem.* **2009**, *48*, 557–564.

(24) Macfarlane, R. M.; Shelby, R. M. In *Spectroscopy of Solids Containing Rare Earth Ions*; Kaplyanskii, A. A., Macfarlane, R. M., Eds.; North-Holland: Amsterdam, 1987; Vol. 51.

(25) Frey, S. T.; Horrocks, W. De W. *Inorg. Chim. Acta* **1995**, *229* 383–390.

(26) Auzel, F.; Dexpert-Ghys, J.; Gautier, C. *J. Lumin.* **1982**, *27*, 1–12.

(27) Benhamou, R. A.; Bessière, A.; Wallez, G.; Viana, B.; Elaatmani, M.; Daoud, M.; Zegzouti, A. *J. Solid State Chem.* **2009**, *182*, 2319–2325.